



Nanoscale

**Design of Nanoconstructs that Exhibit Enhanced Hemostatic Efficiency and Bioabsorbability**

Journal:	<i>Nanoscale</i>
Manuscript ID	NR-MRV-04-2022-002043.R1
Article Type:	Minireview
Date Submitted by the Author:	23-Jun-2022
Complete List of Authors:	Eissa, Rana; Badr University in Cairo Saafan, Hesham; Badr University in Cairo Ali, Aliaa; University of Turku, Chemistry Ibrahim, Kamilia; Ain Shams University Eissa, Noura; Zagazig University Faculty of Pharmacy Hamad, Mostafa; Assiut University Faculty of Medicine Pang, Ching; Texas A&M University, Chemistry Guo, Hongming; Texas A&M University, Materials Science & Engineering Gao, Hui; Tiangong University Elsabahy, Mahmoud; Texas A&M University, Wooley, Karen; Texas A&M University, Chemistry

SCHOLARONE™  
Manuscripts

## Tutorial article

## Design of Nanoconstructs that Exhibit Enhanced Hemostatic Efficiency and Bioabsorbability

Rana A. Eissa<sup>1</sup>, Hesham A. Saafan<sup>1</sup>, Aliaa E. Ali<sup>2</sup>, Kamilia M. Ibrahim<sup>3</sup>, Noura G. Eissa<sup>1,4</sup>, Mostafa A. Hamad<sup>5</sup>,

Received 00th January 20xx,  
Accepted 00th January 20xx

DOI: 10.1039/x0xx00000x

Ching Pang<sup>6</sup>, Hongming Guo<sup>6</sup>, Hui Gao<sup>7\*</sup>, Mahmoud Elsabahy<sup>1, 6, 8\*</sup> and Karen L. Wooley<sup>6\*</sup>

### Abstract

Hemorrhage is a prime cause of death in civilian and military traumatic injuries, whereby a significant proportion of death and complications occur prior to paramedic arrival and hospital resuscitation. Hence, it is crucial to develop hemostatic materials that are able to be applied by simple processes and allow control over bleeding by inducing rapid hemostasis, non-invasively, until subjects receive necessary medical care. This *tutorial* review discusses recent advances in synthesis and fabrication of degradable hemostatic nanomaterials and nanocomposites. Control of assembly and fine-tuning of composition of absorbable (*i.e.*, degradable) hemostatic supramolecular structures and nanoconstructs have afforded the development of smart devices and scaffolds capable of efficiently controlling bleeding while degrading over time, thereby reducing surgical operation times and hospitalization duration. The nanoconstructs that are highlighted have demonstrated hemostatic efficiency pre-clinically in animal models, while also sharing characteristics of degradability, bioabsorbability and presence of nano-assemblies within their compositions.

### Keywords:

Degradable, absorbable, hemostatic materials, nanoconstructs, hemostasis

### Introduction

Uncontrolled hemorrhage is the leading cause of preventable death after injury, particularly if it is not controlled efficiently within the first few minutes to hours. In both civilian and military injuries, uncontrolled hemorrhage accounts for > 40% of preventable deaths. According to the World Health Organization (WHO), 20-50 million people are injured or disabled globally in road traffic accidents each year.<sup>1</sup> Hemorrhage results in blood loss from the cardiovascular system, and subsequently, leads to inappropriate tissue oxygenation and hemorrhagic shock. Hemostasis, a normal physiological process, occurs spontaneously to stop bleeding at the site of injury while preserving normal blood circulation.<sup>2,3</sup>

Health care professionals have explored various methods to aid in the hemostasis process, starting from application of pressure, followed by ligation, cauterization, usage of medical vasoconstrictors, drugs, and dressings.<sup>4</sup> The usage of local hemostatic agents has recently received great interest, although it is a concept that has been used in various ways by many cultures. The ancient Egyptians used barley, wax and grease mixtures to control hemorrhage.<sup>5,6</sup> The old Greek nations applied herbal hemostatic agents to wounds on the battlefield.<sup>5-7</sup> Recent advances in synthetic polymer chemistry and biotechnology have led to development of hemostatic agents that are widely available to health care practitioners.<sup>8-13</sup> These hemostatic agents may be classified as

<sup>1</sup>School of Biotechnology and Science Academy, Badr University in Cairo, Badr City, Cairo 11829, Egypt

<sup>2</sup>Department of Chemistry, University of Turku, Vatselankatu 2, 20014 Turku, Finland

<sup>3</sup>Department of Pharmacology, Faculty of Pharmacy, Ain Shams University, Cairo 11561, Egypt

<sup>4</sup>Department of Pharmaceutics and Industrial Pharmacy, Faculty of Pharmacy, Zagazig University, Zagazig 44519, Egypt

<sup>5</sup>Department of Surgery, Faculty of Medicine, Assiut University, Assiut 71515, Egypt

<sup>6</sup>Departments of Chemistry, Chemical Engineering, and Materials Science & Engineering, Texas A&M University, College Station, Texas 77842, USA

<sup>7</sup>State Key Laboratory of Separation Membranes and Membrane Processes, School of Materials Science and Engineering, Tiangong University, Tianjin 300387, P. R. China

<sup>8</sup>Misr University for Science and Technology, 6<sup>th</sup> of October City, Cairo 12566, Egypt

\*Corresponding authors: [huigao@tiangong.edu.cn](mailto:huigao@tiangong.edu.cn); [wooley@chem.tamu.edu](mailto:wooley@chem.tamu.edu); [mahmoud.elsabahy@buc.edu.eg](mailto:mahmoud.elsabahy@buc.edu.eg)

bioabsorbable and non-bioabsorbable, based on whether the body is able to naturally absorb the dressing. The bioabsorbable processes may include various enzymatic, metabolic and/or hydrolytic degradation reactions, which can occur for partial structural components (*e.g.*, cleavage of linkages along polymer backbones, within cross-linking sites, or for side chain subunits) that transform insoluble polymers to water soluble derivatives, or may simply involve dissolution and clearing of matrix materials as macromolecules. Absorbable hemostats are more appropriate for use in surgical and interventional procedures, as their application shortens the duration of surgery and potentially eliminates the necessity of dressing removal subsequently, unlike non-absorbable hemostats, which may cause bleeding and tissue damage during later removal from the injury site.<sup>14–18</sup>

There is an increasing interest in exploiting various synthetic approaches and macromolecular assembly in construction of efficient hemostatic nanocomposites with degradable backbones, to control their physicochemical properties and achieve the ability to interact with blood components for quick and efficient hemostasis.<sup>8,19,20</sup> Beyond the chemical composition of the hemostatic materials, other parameters of importance include the dimensionality and morphology. For instance, the overall particle or fiber size and shape, including the presence of micro- and nanoscopic features, surface area, surface and sub-surface chemistries, mechanical strength, and malleability play major roles in dictating the hemostatic efficiencies of hemostatic composite materials.

## Hemostatic Nanocomposites: Mechanism and Bioabsorption

Nanocomposite refers to a multiphase solid material comprised of several phases where at least one of them has one dimension in the nanometer range.<sup>21</sup> Different nanomaterials can be included in preparation of these composites such as nanofibers and nanoparticles. A wide variety of hemostatic agents has been incorporated into nanostructures and demonstrated high hemostatic efficiency. Those hemostatic agents act *via* different mechanisms. For example, chitosan, a positively charged polysaccharide of natural origin, interacts with the negatively charged thrombocytes and erythrocytes.<sup>18</sup> This allows for adherence at the bleeding site and aids in platelet aggregation, thus, resulting in the formation of blood clots.<sup>22</sup> Kaolin is aluminum silicate that activates the intrinsic pathway of coagulation by concentrating clotting factors *via* rapid absorption of the water content of blood at the bleeding site.<sup>18</sup> Kaolin also promotes the coagulation process through the activation of the coagulation factor XII and the platelet-associated factor XI, thus initiating the intrinsic clotting pathway and allowing for the formation of a fibrin clot.<sup>23</sup> Sources of calcium are occasionally included in the hemostatic composites to improve their ability to control bleeding. Calcium ions possess a fundamental role in the coagulation process by acting as a cofactor and a linker in various enzymatic processes.<sup>24</sup> Calcium ions are responsible for the complete activation of coagulation factor XIII which covalently crosslinks the preformed fibrin clots thus preventing premature fibrinolysis.<sup>25</sup> Incorporation of these hemostatic agents on the nanoscale provides higher specific surface area and greater chance for interaction with blood components which results in a high

hemostatic efficiency. Furthermore, their assembly on a nanoscale may facilitate their bioabsorbability *in vivo*. For instance, chitosan forms large aggregates in physiological milieu because it requires acidic conditions for dissolution. Nanoscale assembly of chitosan has shown to prevent aggregate formation in physiological environment.<sup>8</sup>

Several of the commercially-available and preclinically-tested hemostatic dressings are degradable and resorbable. Current research studies focus on evaluation of hemostatic efficiency (*i.e.*, blood loss and time to hemostasis), animal survival after injury and biocompatibility of hemostatic materials and technologies. However, studies that report *in vivo* degradation, clearance and trafficking of hemostatic nanocomposites and their degradation products after *in vivo* administration are scarce.<sup>26,27</sup> Further studies should consider the biodegradation/resorption pathways, clearance and elimination kinetics of resorbed hemostat and their degradation products. Development of hemostatic nanoconstructs that possess high hemostatic efficiency while ensuring systemic safety is crucial for success of these nanomaterials.

This *tutorial* review discusses advances in the design and fabrication of recently developed absorbable and degradable hemostatic nanocomposites. Nanoconstructs that have demonstrated hemostatic efficiency pre-clinically in animal models, and share characteristics of degradability and the presence of nanoassemblies within their compositions, are highlighted. Degradable/absorbable hemostatic nanoconstructs discussed in this review are classified into nanofibers, nano-sponges, nanoparticles (Fig. 1), and other more complex morphologies.

## Hemostatic Nanofibers

Nanofibers, commonly prepared *via* electrospinning, have been exploited extensively for the preparation of wound dressings, and as scaffolds for tissue engineering and drug delivery applications.<sup>28–30</sup> Chitosan and gelatin are commonly utilized to form nanofibers for hemostatic and antimicrobial applications. Chitosan is renowned for its high hemostatic activity and, in combination with protection against bacteria, affords rapid wound healing.<sup>31,32</sup> In an attempt to improve hemostatic efficiency of chitosan, blending with gelatin was carried out prior to electrospinning to allow formation of chitosan-gelatin (Cs-Gel) nanofiber mats.<sup>33</sup> *In vitro*, Cs-Gel nanofibers resulted in higher blood clotting efficiencies in rabbit whole blood as compared to chitosan nanofibers. The field emission (FE)-scanning electron microscope (SEM) images of Cs-Gel nanofiber mats showed bead-free structural features with an average diameter of *ca.* 270–300 nm, and the diameter increased as the gelatin concentrations increased in the mixed electrospinning solutions. Interestingly, enhancement in nanofiber porosity by ultra-sonication further improved blood clotting efficiency, explained by increased deposition of platelets and their infiltration into nanofibers having high porosity. Hence, blending of chitosan with other polymers, and controlling porosity of nanofibrous mats may play important roles in dictating hemostatic efficiency.

Chemical modifications to chitosan have also been explored. For instance, tissue adhesives made of a pyrogallol-functionalized chitosan-based hydrogel were fabricated.<sup>19</sup> The amidation-based conjugation of pyrogallol improved the solubility and adhesiveness

of chitosan and combined the hemostatic activity of chitosan with the advantageous properties of gallic acid, which has been shown to possess anti-inflammatory, angiogenic, antioxidant, and antimicrobial properties. Chitosan-gallic acid nanofiber mats were prepared *via* electrospinning at an average fiber diameter of  $700 \pm 100$  nm with no bead formation. Blood clotting efficiency was monitored quantitatively on human blood *via in vitro* blood clotting index (BCI), where the chitosan-gallic acid film showed superior hemostatic efficiency to chitosan and gauze. Furthermore, the chitosan-gallic acid film led to immediate coagulation upon contact with blood, which was attributed to interactions of hydroxyl and amino groups of the chitosan backbone and phenolic groups of the pyrogallol moieties with the biological interface.

Chitosan and chitosan derivatives have been co-fabricated into nanofibers and nanofiber mats together with various natural, modified natural or synthetic polymers to achieve multiple biological outcomes. In one example, Yin *et al.* developed dual hemostatic and antimicrobial nanofibrous membranes based on quaternary ammonium-modified chitosan (CSENDMH), blended with poly(vinyl alcohol) (PVA), and electrospun to afford PVA/CSENDMH nanofibrous materials.<sup>34</sup> SEM images displayed smooth and uniform bead-free morphologies, indicating homogeneous blending, with average nanofiber diameters reduced from 195 nm for PVA to 135 nm upon the addition of CSENDMH to PVA solution. Further, *N*-halamine chlorinated analogs PVA/CSENDMH-Cl were prepared by immersing the fibrous membranes in a 10% aqueous household bleach solution for 1 h. The chlorinated PVA/CSENDMH-Cl formed dense porous membranes of smaller nanofibrous diameters. Human blood coagulation was assessed by BCI, the lower the BCI, the higher the hemostatic capacity of the materials. The PVA, PVA/CSENDMH and PVA/CSENDMH-Cl membranes each showed significantly lower BCI compared to the control, however, the chitosan derivatives, either chlorinated or not, had lower BCI values in comparison to PVA-only membranes. In addition, the nanofibrous membranes had the ability to entrap and aggregate red blood cells and platelet components into their network to form clots. As expected, based upon the presence of quaternary ammonium and halogenated groups,<sup>35</sup> incorporation of the modified chitosan components afforded > 97% antibacterial activities against *S. aureus* and *E. Coli* O157:H7 within minutes.

Sasmal *et al.* fabricated hemostatic patches with ternary antifibrinolytic, antibacterial and hemostatic properties.<sup>36</sup> PVA as a basic material was mixed with the hemostatic and antibacterial polymer, chitosan at different PVA:chitosan ratios (3:2 and 1:1) by electrospinning. For drug-loaded electrospun patches, the antifibrinolytic agent known as tranexamic acid (TXA) was added to the PVA powder prior to the electrospinning process. It was found that the diameter of the membranes decreased upon increasing chitosan content and increased upon addition of TXA. The diameters were 180 and 150 nm for the ratios 3:2 and 1:1 (PVA:chitosan), respectively, while the diameters were 220 and 160 nm in the presence of TXA, respectively. To assess the hemostatic efficacy, the blood clotting time (CT) of TXA-loaded and non-loaded nanofibers were measured after collecting the blood sample from a healthy volunteer. The CT of the ratios 3:2 and 1:1 were 217 and 187 s, respectively, which were significantly lower than that with the control. The CT in the presence of TXA was lower than the non-drug-

loaded patches at both ratios. Although the difference between the TXA-loaded and non-loaded patches at the 3:2 ratio was insignificant, there was a significant difference between the 2 patches at the 1:1 ratio. Overall, the addition of TXA resulted in a significant reduction in the CT to *ca.* 82% and 65% at the ratios of 3:2 and 1:1, respectively. All CT of the sample patches were significantly reduced when compared to controls.

Park *et al.* used polycaprolactone (PCL), calcium carbonate and  $\beta$ -chitosan to prepare hemostatic nanofiber mats *via* electrospinning.<sup>37</sup> PCL has the advantage of being a polyester that is hydrolytically degradable, vs. the non-degradable backbone of PVA. The authors used PCL as a carrier for artificial calcium carbonate ( $\text{CaCO}_3$ ) that was synthesized from calcium chloride and sodium carbonate.  $\text{CaCO}_3$  was then added to the fiber solution to allow for the formation of PCL/ $\text{CaCO}_3$  nanofibers. Nanofibers were coated with  $\beta$ -chitosan as a hemostatic polymer *via* an ultrasonic spray coating method. PCL has unique physical properties, such as a relatively low melting point, low cost, biodegradability, and high blending compatibility. Nevertheless, PCL provides low wettability due to its hydrophobic nature.  $\beta$ -chitosan was incorporated as a hydrophilic polymer to improve wettability and to increase the surface area, thus facilitating blood permeation into the fibers. Moreover,  $\beta$ -chitosan is well-known for its wound healing properties.  $\text{CaCO}_3$  plays a role in the coagulation process by releasing calcium ions that promote formation of blood clots. PCL and PCL/ $\text{CaCO}_3$  nanofibers had diameters in the range of 500 nm–1  $\mu\text{m}$ , as demonstrated by FE-SEM. Clotting of whole pig blood treated with PCL, PCL/ $\text{CaCO}_3$  and PCL/ $\text{CaCO}_3$ / $\beta$ -chitosan nanofibers was investigated. PCL nanofibers showed similar results to that of a conventional gauze, whereas PCL/ $\text{CaCO}_3$  nanofibers exhibited better results than gauze, confirming the role of  $\text{CaCO}_3$  in promoting coagulation. Furthermore, the PCL/ $\text{CaCO}_3$  nanofiber sprayed with  $\beta$ -chitosan presented the best clotting rate among all samples, which was attributed to the ability of  $\beta$ -chitosan to electrostatically interact with blood components and enhance the aggregation of the red blood cells. Similar results were observed using whole mouse blood.

Beyond the use of chitosan, Li *et al.* have developed organic-inorganic hybrid hemostatic nanofibrous mats of antibacterial activity by incorporating curcumin-loaded mesoporous silica nanoparticles (CCM/MSNs) into polyvinylpyrrolidone (PVP) *via* electrospinning (Fig. 2).<sup>38</sup> PVP is a water-soluble polymer that can be rapidly converted to a hydrogel, whereas MSNs are biocompatible nanocarriers that can be loaded with the antibacterial curcumin. The MSNs were functionalized with amine groups prior to curcumin loading to facilitate intermolecular interactions between the amine groups and the polar groups of curcumin. Curcumin-loaded MSNs were well-distributed within the fiber mats with no bead defects. The cytotoxicity of materials was tested by measuring the viability of murine L929 fibrosarcoma cells (L929) by using the CCK-8 method in which nanofibers showed no sign of toxicity to L929 cells after 1 d and 3 d of incubation. The *in vitro* antibacterial activity was assessed by measuring the diameter of the inhibition zone in which CCM/MSNs-PVP showed persistent antibacterial activity. The results indicated that neat PVP and 4% MSNs-PVP did not show an inhibition zone, whereas 2, 4, 8% CCM/MSNs-PVP nanofibers showed inhibition zones of 10.6, 10.8, and 11.4 mm, respectively, after 48-h incubation. The hemostatic efficiency was evaluated *in vitro* by

testing fresh rat blood absorption efficiency of the mats. Upon contact with blood, CCM/MSNs-PVP nanofiber mats formed a hydrogel composite (Fig. 2c) that showed a maximum whole blood absorption ratio of 300% of the weight compared with only 150% in the hemostatic gauze. The high-water adsorption capacity helps to concentrate blood cells and cause aggregation of platelets, thereby, promoting clot formation. The coagulation times observed for MSNs-PVP nanofibers in prothrombin time and activated partial thromboplastin time tests were remarkably reduced, in comparison to the control. The effect was also dependent on the concentration of the added materials. The hemostatic efficacy was explored *in vivo* using a liver injury experiment on male ICR mice as the animal hemorrhage model. The hemorrhagic model was treated with 4 wt% CCM/MSNs-PVP hybrid nanofibers and rapid hemostasis was achieved after formation of the hydrogel composite. Furthermore, none of the mice was infected prior to the complete wound healing.

Shefa *et al.* incorporated zinc oxide (ZnO) in 2,2,6,6-tetramethylpiperidine-1-oxyl (TEMPO)-oxidized cellulose nanofibers (TOCN) and poly(ethylene glycol) (PEG) through freeze drying, to afford formation of hemostatic fibers that possess antibacterial properties.<sup>39</sup> *In vivo* evaluation of the hemostatic composites was carried out in a rabbit ear arterial bleeding model. Incorporation of ZnO and higher percentages of PEG (*i.e.*, 10%) reduced the swelling of the nanofibers and shortened the bleeding time in the rabbit ear injury model. ZnO imparted antibacterial properties to the dressing, particularly against Gram positive bacteria.

Liu *et al.* fabricated and deposited bifunctional copper monosulfide (CuS) composite nanofibers directly into wound sites *via* an *in situ* green method that employed a portable electrospinning device to achieve rapid hemostasis and ablate superbugs simultaneously.<sup>40</sup> The electrospun nanofibers, comprised of CuS nanoparticles (*ca.* 10 nm), gelatin and PVP, showed a porous network of 400 nm diameter fibers with a narrow size distribution, as demonstrated by SEM and transmission electron microscopy (TEM) (Fig. 3). *In vitro* human blood clotting assays indicated that the nanofiber membranes had higher clotting effects than medical gauze control samples, probably due to the smaller pore size that enabled platelet aggregation more rapidly and effectively. Furthermore, the photothermal activity of CuS composite nanofibers could kill Gram-negative bacteria of *E. coli* and Gram-positive bacteria of methicillin-resistant *S. aureus*. *In vivo* experiments were carried out to evaluate the simultaneous hemostatic and antibacterial activities using rats in which the incision was inoculated with super-bacterial infection of *P. aeruginosa*. The nanofibers resulted in acceleration of hemostasis (< 6 s) and reduced the wound healing time (18 d). This study was a good example of the need for design of multifunctional nanocomposites for achieving hemostasis and efficient wound healing, whereby hemostatic activity was accomplished *via* the hemostatic properties of the nanofibers, while antibacterial activity was achieved through the photothermal activity of CuS.

Composites of degradable polymers with bioactive additives have also been pursued. In one case, Wyrwa *et al.* developed novel hemostatic materials based on poly(L-lactide-co-D,L-lactide) (PLA) loaded with different concentrations of adrenaline (AD10% or AD20% w/w) and TXA (20% or 50% w/w) *via* electrospinning.<sup>41</sup> These fabrics are biocompatible, thin and flexible, and have demonstrated average fiber diameters of *ca.* 385–715 nm. The fibers were

extensively characterized, and based on their physicochemical characteristics and cytotoxicities, PLA-AD10 and PLA-TXA20 were selected for further *in vivo* studies. The electrospun fabrics were tested on a nasal injury rabbit model and amounts of blood loss were measured to evaluate the hemostatic efficacy. Application of the PLA fibers reduced the amount of blood loss to 48 mg, compared to 58 mg in animals that were not treated. The PLA-AD10 and PLA-TXA20 reduced the amounts of blood loss to 15 and 30 mg, respectively.

Even simpler compositions have been explored to achieve fiber formation *via* supramolecular assembly, coincident with in-built enzymatic stability and hemostatic activity *via* the use of D-amino acid peptide oligomers. For instance, Luo *et al.* developed 3-dimensional nanofiber scaffolds through the self-assembly of D-amino acids (D-EAK16).<sup>42</sup> The hemostatic efficiency of the scaffold was examined against rabbit erythrocyte solution to evaluate the coagulation activity *in vitro*. Peptides were able to induce agglutination, and the effect was concentration-dependent. Similar results were obtained in four different types of human blood. Moreover, *in vivo* examination was performed in a rabbit liver wound healing model, which indicated that 1% of D-EAK16 and L-EAK16 resulted in blood clotting after *ca.* 20 and 17 s, respectively. Hence, both D-EAK16 and L-EAK16 can self-assemble into hemostatic nanofibers that are able to control bleeding, although the non-natural “D” stereoisomer resists protease degradation and, thus, was considered to be more suitable for clinical use.

## Hemostatic Nanoparticles

In comparison to composite hemostatic materials that contain nanofibers, short aspect ratio nanoparticles have also been studied extensively, as active agents in solution, as lyophilized powders or as additive components to micro-to-macroscopic composites that have led to remarkable hemostatic performances, and/or made contributions to the composition, structure, morphology and properties of hemostatic composite materials. For instance, Luo *et al.* developed keratine nanoparticles *via* a modified emulsion diffusion method,<sup>43</sup> to investigate their performance as a unique form of keratin biomaterials, which have shown efficacy in hemostasis, wound healing and tissue repair.<sup>44–46</sup> *In vitro* blood clotting assays indicated that keratine extracts and keratine nanoparticles significantly reduced blood clotting times from 585 s in the control group (*i.e.*, with no additives), to *ca.* 85 and 45 s, respectively in a fresh rat blood sample. *In vivo* studies were performed in two animal models, rat liver puncture and rat tail amputation. In the rat liver puncture assay, keratine extracts and keratine nanoparticles reduced blood loss by 300% and 400%, respectively, and reduced the time to hemostasis by 150% and 250%, respectively. Similarly, in the rat tail amputation model, keratine extracts and keratin nanoparticles reduced mass blood loss and time to hemostasis with superior effects observed in the case of keratine nanoparticles.

MSNs are good candidates for hemostatic processes, owing to their high specific surface area, pore structure and good biocompatibility.<sup>47</sup> Chen *et al.* modified MSNs by adding chitosan and hydrocaffeic acid (MSNs/Cs-HCA) for a rapid and safe hemorrhage control. Chitosan is well-known for its hemostatic properties, while negative charges of the catechol groups of HCA trigger clotting factor

XII, thereby initiating coagulation cascades. Furthermore, catechol groups impart tissue adhesion properties to MSNs. The coagulation efficacy was tested by measuring the hemoglobin absorbance of the whole rat blood before and after treatment. The absorbance of MSNs, MSNs/Cs and MSNs/Cs-HCA samples decreased over time, however, the clotting efficiency of MSNs/Cs-HCA samples were superior to MSNs and MSNs/Cs. These results indicate the ability of the three samples to promote blood clotting and highlight the synergistic effect provided by HCA. For further *in vivo* evaluation, a rat liver laceration was performed. The MSNs, MSNs/Cs and MSNs/Cs-HCA displayed hemostatic times that were 34.6%, 50.9% and 62.6% shorter than that of the control group, respectively. A femoral artery rat model was also tested. The hemostatic rates of MSNs, MSNs/Cs and MSNs/Cs-HCA were 18.7%, 61.4% and 67.7% faster than that of the control group, respectively.

Liu *et al.* exploited amorphous silica nanoparticles coated with polydopamine (PDA/SiNP) that formed a porous network after lyophilization.<sup>48</sup> Phenolic hydroxyl and amino groups in the hydrophobic domain aid in activation of the coagulation system and accelerate the wound healing process. PDA/SiNP showed *ca.* 50% reduction in the clotting time compared to the commercial Celox™. *In vivo* hemostatic activity of PDA/SiNP was evaluated in two rat models. In a lethal femoral artery and vein injury model, PDA/SiNP displayed comparable results to Celox™ in terms of time to hemostasis (*i.e.*,  $104 \pm 11$  s and  $109 \pm 8$  s, respectively). However, a significant reduction in blood loss was achieved in the case of PDA/SiNP (1.4 g), compared to Celox™ (3.8 g) and the conventional gauze (4.7 g). In a severe liver injury model, PDA/SiNP and Celox™ achieved rapid hemostases of 86 and 102 s, respectively, compared to the control groups. Moreover, PDA/SiNP resulted in 68% reduction in blood loss compared to Celox™. Worth mentioning is that the PDA/SiNP exhibited sustained antibacterial activity against *E. coli*.

A nano-dressing composed of chitosan-pectin-titanium dioxide (TiO<sub>2</sub>) was prepared by Archana *et al.* to evaluate its antibacterial activity and *in vivo* wound healing capacity.<sup>49</sup> *In vitro* antibacterial assays demonstrated superior antibacterial activity of the chitosan-pectin-TiO<sub>2</sub> nano dressing against several microbial strains (*i.e.*, *E. coli*, *S. aureus*, *P. aeruginosa*, *B. subtilis* and *A. niger*). These results were attributed to electrostatic interactions between the positively-charged dressings and negatively-charged bacterial membranes, in combination with accelerated rates of antibacterial action from the high surface area of nanosized TiO<sub>2</sub>. In an *in vivo* open excision-type wound rat model, wound closure rate was observed in rats treated with chitosan-pectin-TiO<sub>2</sub> nano-dressing, chitosan, or gauze over 16 d. At the end of the experiment (*i.e.*, after 16 d), 99% wound healing was observed for animals treated with chitosan-pectin-TiO<sub>2</sub> nano-dressing, while *ca.* 95% and 91% wound closure rates were observed in the cases of chitosan and gauze, respectively.

## Hemostatic Nanosponges

Nanosponges are soft and flexible macroscopic materials, which contain interesting nanoscopic features, and are insoluble in water and organic solvents. They are porous, and stable at a temperatures up to 300 °C.<sup>50</sup> Nanosponges allow for entrapment of various cargoes

within their internal domains, owing to their three-dimensional structures that contain cavities of nanometric sizes and polarities. Nanosponges could be made of biodegradable backbones, which is an important advantage in the design of hemostatic nano-dressings. Synthesis of nanosponges is much easier than the manufacturing of nanofibers. In the solvent method, polymers are mixed with crosslinkers in an appropriate solvent under a specific temperature. Another method is ultrasound-assisted synthesis, where polymers and crosslinkers are mixed in the absence of solvents under sonication.

Tan *et al.* prepared porous chitin nanofiber sponges through a freeze-drying process, followed by surface modification and coating with tannic acid/Ca<sup>2+</sup> via a layer-by-layer deposition method.<sup>51,52</sup> Chitin is a natural biopolymer that can be utilized for the preparation of hemostatic agents due to its antibacterial effect, biodegradability, and biocompatibility. Tannic acid, a naturally occurring polyphenol, possesses hemostatic, antibacterial and antioxidant properties. *In vivo* studies of the hemostatic nanosponges were evaluated in two models, rat tail amputation and rat liver laceration. In both models, tannic acid/Ca<sup>2+</sup>-chitin nanofiber sponges significantly shortened the times to hemostasis compared to the unmodified chitin nanofiber sponges or the conventional medical gauze. These results were attributed to the enhanced blood captured on the surface modified-chitin nanofiber sponges in addition to the essential role of Ca<sup>2+</sup> in platelet activation. Tannic acid/Ca<sup>2+</sup>-chitin nanofiber sponges displayed good hemocompatibility, whereas the presence of tannic acid in the surface-modified nanosponges enhanced the antibacterial effect of the sponge, and the effect was concentration-dependent.

Gao *et al.* developed a combination of a porous sponge of carboxylated brown algae cellulose nanofibers (BACNFs) and an antibacterial quaternized β-chitin (QC) intercalated into the interlayer space of the organic rectorite (OREC) to afford the formation of a composite suspension (QCRs) via electrostatic interactions.<sup>53</sup> The BACNFs sponge was soaked in the QCRs suspensions to form the BACNFs/QCRs through a freeze-dry process. The antibacterial activities were examined by observing the inhibition zones for the BACNFs/QCRs and BACNFs against *E. coli* and *S. aureus*. Unlike BACNFs/QCRs, BACNFs did not demonstrate clear inhibition zones for both types of bacteria. BACNFs, QC and OREC reduced coagulation time in comparison to the conventional gauze when applied to rats after a tail amputation. Wounds covered by BACNFs/QCRs were completely healed after 12 d compared to the wounds covered with conventional gauze that were healed after 15 d. Histological examination demonstrated a lower level of inflamed cells in the BACNFs/QCRs-treated wounds than those in the conventional gauze group. The levels of vascular endothelial growth factor (VEGF) and VEGF receptors were higher in the group treated with BACNFs/QCRs compared to the gauze group after 9 d.

Yan *et al.* synthesized chitosan/calcium pyrophosphate nanoflowers (CPNFs) through an improved one-pot preparation method (Fig. 4).<sup>54</sup> The CPNFs were then mixed with collagen to form CPNFs-Col sponge via freeze drying. Biocompatibility of the CPNFs-Col sponge was assessed via intracutaneous stimulation test, and a series of hemolysis, acute systemic toxicity, and cytotoxicity assays. The synthesized nanosponges showed no signs of pathological reactions or hemolysis, and no signs of altered mice behavior (*i.e.*,

slow movement or reduced food intake) were observed for three days after administration. *In vivo* hemostatic efficiencies were evaluated in a rabbit hepatic trauma model and an ear artery model. CPNFs-Col sponge revealed the strongest hemostatic activity with the shortest clotting time and the least amount of blood loss compared to the collagen sponge, chitosan sponge and conventional gauze. In the thigh muscle of New Zealand white rabbits, CPNFs-Col sponge degraded into small fragments in the first 14 d, which were completely absorbed after 21 d, with no redness or swelling at the site of implantation.

## Hemostatic Nanobioglasses

Nanobioglasses (nBG) incorporate similar concepts as nanoparticles and nanosponges, yet typically are comprised of inorganic matrices that exhibit glass-like rigidity and contain cavities into which organic materials may be packaged.<sup>55</sup> Indeed, nBGs include MSNs among other compositions, including the incorporation of calcium oxide to achieve hemostatic character driven both by high surface area of intact nBGs and release of calcium ions during nBG degradation and bioabsorption. The incorporation of organic additives further enhances the synergistic effects, resulting in highly effective hemostatic composites. For instance, Chen *et al.* fabricated mesoporous bioglass nanoparticles (mBGN, 70SiO<sub>2</sub>-30CaO in mol%) through a sol-gel method,<sup>56</sup> and then loaded carboxymethyl starch and chitosan oligosaccharide polyelectrolyte complexes (PEC) (10 and 20 wt%) *via in situ* coprecipitation followed by lyophilization to form BGN/PEC. PECs exhibit good hemostatic activities and biocompatibility<sup>57</sup> while bioglass possesses enhanced blood coagulation capacity. The hemostatic properties of bioglass are due to the release of Ca<sup>2+</sup> ions which play a critical role in the coagulation cascade. Furthermore, the highly negative charge of the bioglass surface activates the intrinsic pathway of coagulation cascade.<sup>58</sup> *In vitro* coagulation was evaluated, and BGN/PEC showed an enhanced fresh rat blood clotting rate compared to the control, and the effect was further improved upon increasing mBGN content (20 wt%). The hemostatic activity was also evaluated *in vivo* in a rabbit hepatic hemorrhage model. Blood clotting times in groups treated with 10 wt% BGN/PEC and 20 wt% BGN/PEC were 39 s and 36 s, respectively, indicating that the hemostatic activity was concentration-independent. However, lower blood loss was observed in the case of 10 wt% BGN/PEC.

Sundaram *et al.* synthesized biocompatible nBG through a sol-gel method followed by incorporation of chitosan to form a chitosan-nBG composite hydrogel.<sup>59</sup> *In vitro* coagulation was studied on rat model, and the blood clotting time was recorded. Normal blood clotted after 462 ± 16 s. Blood clotting time was 350 ± 15 s after applying chitosan hydrogel, while the blood clotting time was 212 ± 21 s after treatment with the chitosan-nBG nanocomposite hydrogel. *In vivo*, in a rat liver injury model, blood clotting times were 132 ± 5, 75 ± 3 and 54 ± 3 s in control (*i.e.*, untreated) animals, after application of chitosan hydrogel and chitosan-nBG composite hydrogel, respectively. The mass of blood loss was also significantly reduced after applying the nanocomposites compared to the chitosan hydrogel. Similar results were also observed in a femoral artery injury model.

## Hemostatic Hierarchically Hybrid Morphologies

Hierarchically hybrid composites include structures of higher orders that are assembled from various components (*e.g.*, organic and inorganic) to allow assembly of hemostatic agents into specific morphologies (*e.g.*, honeycomb-like nanostructures) with features ranging from nanoscale to macroscale.<sup>21</sup> Porous organic matrices offer a breadth of compositions, structures, morphologies and properties to serve as degradable scaffolds for loading of composite components in the creation of hierarchical hybrid morphologies. These morphologies are capable of segregating hemostatic materials to optimize both their blood clotting ability and biodegradability. For instance, chitosan is highly effective in blood clotting and possesses antimicrobial characteristics, but chitosan powder is not considered a bioabsorbable material, as it forms large aggregates and requires acidic media for dissolution. As a result, it is necessary to mechanically remove chitosan powder/aggregates from wounds prior to surgery. Therefore, chitosan is typically loaded onto non-degradable materials (*e.g.*, gauze) when used as an active component in many commercial dressings, such as, HemCon<sup>®</sup>, Chitodine<sup>®</sup>, TraumaDEX<sup>®</sup>, and Celox<sup>™</sup>. When these products are applied internally, an extra procedure is required for bandage removal, resulting in potential bleeding and tissue damage. Leonhardt *et al.* have developed a nanoporous/nanofibrous hybrid morphology with distinct domains comprised of a degradable template into which was intercalated an inverse nanoporous chitosan – individually addressable and uniquely degradable/extractable, dually bioabsorbable.<sup>8</sup> By this process, hemostatic chitosan-based nanofibers were assembled within the macroporous carrier of β-cyclodextrin polyester (CDPE-Cs) hydrogel. CDPE is a sacrificial template that degrades over time under physiological conditions. The template allowed assembly of imprinted chitosan into extensively entangled nanofibers of macroscopic honeycomb-like monolithic mats with diameters of 9.2 ± 3.7 nm, as viewed by SEM (Fig. 5). Sites capable of ionic interactions within the bioabsorbable CDPE matrix enabled the assembly of the aqueous cationic chitosan solution at high effective surface area. The hemostatic efficiency of CDPE-Cs was tested *in vivo* in acute liver punch models of rabbits, rats, pigs, in comparison to commercially available bioabsorbable Surgicel<sup>®</sup> and Curaspan<sup>®</sup>, and the blank CDPE (Fig. 6). Application of the conventional gauze could not stop the bleeding in the three animal models until the end of the experiment, with significant amounts of blood loss from the injury sites. Surgicel<sup>®</sup> and Curaspan<sup>®</sup> were significantly better than the conventional gauze in reducing the time required to hemostasis and decreasing the amounts of blood loss. As can be seen from Fig. 6, exceptional improvement in hemostatic efficiency, expressed in time of hemostasis and amounts of blood loss, was observed after treatment with the CDPE-Cs in the three animal models, in comparison to the conventional gauze and the commercially available absorbable hemostatic dressings. Worth note is that after implantation of the CDPE-Cs, Surgicel<sup>®</sup>, Curaspan<sup>®</sup>, and blank CDPE in the injured liver of rats for 7 days, no residues were found. Degradation of the biocompatible CDPE sacrificial template, *in vitro* and *in vivo*, was demonstrated. However, the extent to which dissolution vs. metabolism are involved in the biological clearance *in vivo* remains unclear.

## Conclusions and Perspectives

As we reflect upon the highly promising results that have been obtained across a broad range of composite hemostatic materials, this review has highlighted just a few examples, categorized based upon their morphology (*e.g.*, fiber vs. particle), properties (*e.g.*, flexible vs. rigid), compositions (*e.g.*, organic vs. inorganic matrices), with indications of their effectiveness for hemostasis. Advances in synthetic chemistry alongside supramolecular assembly have allowed construction of degradable nanocomposites of high hemostatic efficiency. Recent progress in the synthesis of degradable polymer backbones and design of nanoparticles of diverse morphologies have allowed integration into hemostatic composites.<sup>60–63</sup> However, the types of polymers exploited, shape of nanoscopic features, degradability, and degradation products, might have a great effect on hemostatic efficiency, cyto- and immunotoxicities, and degradation/release kinetics.<sup>64–66</sup> More comprehensive studies should be conducted to achieve safe and effective bioabsorbable hemostatic materials, including identification and screening of the metabolites *in vitro* and *in vivo*. Incorporation of functional polymers, such as chitosan<sup>67</sup> – loaded or not with antibacterial agents – might add benefits for minimizing infections and affording wound healing after hemostasis is achieved. Moreover, by co-fabricating natural materials that exhibit hemostatic and antimicrobial (and other biological effects), such as chitosan, chitin, *etc.*, with organic or inorganic synthetic scaffolds, multiple beneficial biological effects and biodegradabilities have been achieved. Innovative chemistries and clever engineering will be needed to further advance the complexities of the compositions, topologies, and morphologies, especially when there are challenges with solubilities, compatibilities, *etc.* Future hybrid science, engineering and medicine approaches may chart pathways toward tunable physicochemical, mechanical and biological properties for blood clotting and other biological impacts. Furthermore, there is an opportunity for tuning stability and degradation time, especially for use with different tissues having different mechanical properties, dimensions, healing times, *etc.*

## Author Contributions

Conceptualization; M.E.; Data curation; all authors, Writing - original draft; all authors; Writing - review & editing; all authors.

## Conflicts of interest

There are no conflicts to declare.

## Acknowledgments

Support by the National Science Foundation (CHE-2003771 and DMR-1905818) and the Robert A. Welch Foundation through the W. T. Doherty-Welch Chair in Chemistry (A-0001) are gratefully acknowledged.

## References

1. World Health Organization. Road traffic injuries. [https://www.who.int/news-room/fact-sheets/detail/road-](https://www.who.int/news-room/fact-sheets/detail/road-traffic-injuries)

2. traffic-injuries (2021).
2. Pierce, A. & Pittet, J.-F. Practical understanding of hemostasis and approach to the bleeding patient in the OR. *Advances in anesthesia* **32**, 1–21 (2014).
3. Zhao, Y., Zhang, Z., Pan, Z. & Liu, Y. Advanced bioactive nanomaterials for biomedical applications. *Exploration* **1**, 20210089 (2021).
4. Behrens, A. M., Sikorski, M. J. & Kofinas, P. Hemostatic strategies for traumatic and surgical bleeding. *Journal of Biomedical Materials Research Part A* **102**, 4182–4194 (2014).
5. Achneck, H. E. *et al.* A comprehensive review of topical hemostatic agents: Efficacy and recommendations for use. *Annals of Surgery* **251**, 217–228 (2010).
6. Pereira, B. M., Bortoto, J. B. & Fraga, G. P. Topical hemostatic agents in surgery: Review and prospects. *Revista do Colegio Brasileiro de Cirurgioes* **45**, 1–11 (2018).
7. Hollaus, P. H. Military medicine in ancient Greece [1]. *Annals of Thoracic Surgery* **72**, 1793 (2001).
8. Leonhardt, E. E., Kang, N., Hamad, M. A., Wooley, K. L. & Elsbahy, M. Absorbable hemostatic hydrogels comprising composites of sacrificial templates and honeycomb-like nanofibrous mats of chitosan. *Nature Communications* **10**, 1–9 (2019).
9. Li, H. *et al.* Antibacterial, hemostasis, adhesive, self-healing polysaccharides-based composite hydrogel wound dressing for the prevention and treatment of postoperative adhesion. *Materials science & engineering. C, Materials for biological applications* **123**, 111978 (2021).
10. Biranje, S. S. *et al.* Cytotoxicity and hemostatic activity of chitosan/carrageenan composite wound healing dressing for traumatic hemorrhage. *Carbohydrate Polymers* **239**, 116106 (2020).
11. Zhang, S. *et al.* Oxidized cellulose-based hemostatic materials. *Carbohydrate polymers* **230**, 115585 (2020).
12. Zhao, Y. *et al.* Blood-clotting model and simulation analysis of polyvinyl alcohol–chitosan composite hemostatic materials. *J. Mater. Chem. B* **9**, 5465–5475 (2021).
13. Zhu, H. *et al.* Fast and High Strength Soft Tissue Bioadhesives Based on a Peptide Dendrimer with Antimicrobial Properties and Hemostatic Ability. *ACS applied materials & interfaces* **12**, 4241–4253 (2020).
14. Albala, D. M. *et al.* Hemostasis during urologic surgery: fibrin sealant compared with absorbable hemostat. *Reviews in urology* **17**, 25–30 (2015).
15. Jenkins, P., Rogers, L., Coleman, M. & Freeman, S. Ultrasound appearance of SURGICEL® Absorbable Hemostat (oxidised cellulose) following laparoscopic resection of a splenic cyst – A potential diagnostic peril. *Ultrasound* **28**, 124–130 (2020).
16. Miyamoto, H. *et al.* The effects of sheet-type absorbable topical collagen hemostat used to prevent pulmonary fistula after lung surgery. *Annals of Thoracic and Cardiovascular Surgery* **16**, 16–20 (2010).
17. Niu, W. *et al.* Starch-derived absorbable polysaccharide hemostat enhances bone healing via BMP-2 protein. *Acta histochemica* **119**, 257–263 (2017).

18. Elsabahy, M. & Hamad, M. A. Design and Preclinical Evaluation of Chitosan/Kaolin Nanocomposites with Enhanced Hemostatic Efficiency. *Marine Drugs* **19**, 50 (2021).
19. Sanandiya, N. D. *et al.* Tunichrome-inspired pyrogallol functionalized chitosan for tissue adhesion and hemostasis. *Carbohydrate polymers* **208**, 77–85 (2019).
20. Tan, L., Hu, J., Huang, H., Han, J. & Hu, H. Study of multi-functional electrospun composite nanofibrous mats for smart wound healing. *International journal of biological macromolecules* **79**, 469–476 (2015).
21. Omanović-Miklićanin, E., Badnjević, A., Kazlagić, A. & Hajlovac, M. Nanocomposites: a brief review. *Health and Technology* **10**, 51–59 (2020).
22. Radwan-Pragłowska, J. *et al.* Chitosan-Based Bioactive Hemostatic Agents with Antibacterial Properties-Synthesis and Characterization. *Molecules* **24**, 2629 (2019).
23. Gegel, B. *et al.* The effects of QuikClot Combat Gauze and movement on hemorrhage control in a porcine model. *Military Medicine* **177**, 1543–1547 (2012).
24. Dahlbäck, B. Blood coagulation and its regulation by anticoagulant pathways: Genetic pathogenesis of bleeding and thrombotic diseases. *Journal of Internal Medicine* **257**, 209–223 (2005).
25. Singh, S. *et al.* Structure functional insights into calcium binding during the activation of coagulation factor XIII A. *Scientific Reports* **9**, 1–18 (2019).
26. Hickman, D. S. A., Pawlowski, C. L., Sekhon, U. D. S., Marks, J. & Gupta, A. Sen. Biomaterials and Advanced Technologies for Hemostatic Management of Bleeding. *Advanced Materials* **30**, 1–40 (2018).
27. Wang, X. X. *et al.* Recent Advances in Hemostasis at the Nanoscale. *Advanced Healthcare Materials* **8**, e1900823 (2019).
28. Fathi, H. A. *et al.* Electrospun vancomycin-loaded nanofibers for management of methicillin-resistant *Staphylococcus aureus*-induced skin infections. *International Journal of Pharmaceutics* **586**, 119620 (2020).
29. Silva, N. H. C. S. *et al.* Multifunctional nanofibrous patches composed of nanocellulose and lysozyme nanofibers for cutaneous wound healing. *International journal of biological macromolecules* **165**, 1198–1210 (2020).
30. Samadian, H., Mobasheri, H., Azami, M. & Faridi-Majidi, R. Osteoconductive and electroactive carbon nanofibers/hydroxyapatite nanocomposite tailored for bone tissue engineering: in vitro and in vivo studies. *Scientific reports* **10**, 14853 (2020).
31. Jayakumar, R., Prabakaran, M., Sudheesh Kumar, P. T., Nair, S. V & Tamura, H. Biomaterials based on chitin and chitosan in wound dressing applications. *Biotechnology advances* **29**, 322–337 (2011).
32. Gegel, B. *et al.* The Effects of BleedArrest, Celox, and TraumaDex on Hemorrhage Control in a Porcine Model. *Journal of Surgical Research* **164**, e125–e129 (2010).
33. Gu, B. K. *et al.* Gelatin blending and sonication of chitosan nanofiber mats produce synergistic effects on hemostatic functions. *International journal of biological macromolecules* **82**, 89–96 (2016).
34. Yin, M. *et al.* Novel quaternarized N-halamine chitosan and polyvinyl alcohol nanofibrous membranes as hemostatic materials with excellent antibacterial properties. *Carbohydrate Polymers* **232**, 115823 (2020).
35. Chen, Z. & Sun, Y. N-Halamine-Based Antimicrobial Additives for Polymers: Preparation, Characterization and Antimicrobial Activity. *Industrial & engineering chemistry research* **45**, 2634–2640 (2006).
36. Sasmal, P. & Datta, P. Tranexamic acid-loaded chitosan electrospun nanofibers as drug delivery system for hemorrhage control applications. *Journal of Drug Delivery Science and Technology* **52**, 559–567 (2019).
37. Park, J. Y., Kyung, K. H., Tsukada, K., Him, S. H. & Shiratori, S. Biodegradable polycaprolactone nanofibres with beta-chitosan and calcium carbonate produce a hemostatic effect. *Polymer* **123**, 194–202 (2017).
38. Li, D. *et al.* Fabrication of curcumin-loaded mesoporous silica incorporated polyvinyl pyrrolidone nanofibers for rapid hemostasis and antibacterial treatment. *RSC Advances* **7**, 7973–7982 (2017).
39. Shefa, A. A. *et al.* Investigation of efficiency of a novel, zinc oxide loaded TEMPO-oxidized cellulose nanofiber based hemostat for topical bleeding. *International Journal of Biological Macromolecules* **126**, 786–795 (2019).
40. Liu, X.-F. *et al.* Bifunctional CuS composite nanofibers via in situ electrospinning for outdoor rapid hemostasis and simultaneous ablating superbug. *Chemical Engineering Journal* **401**, 126096 (2020).
41. Wyrwa, R. *et al.* Electrospun mucosal wound dressings containing styptics for bleeding control. *Materials Science and Engineering C* **93**, 419–428 (2018).
42. Luo, Z., Wang, S. & Zhang, S. Fabrication of self-assembling d-form peptide nanofiber scaffold d-EAK16 for rapid hemostasis. *Biomaterials* **32**, 2013–2020 (2011).
43. Luo, T. *et al.* Development and assessment of kerateine nanoparticles for use as a hemostatic agent. *Materials Science and Engineering C* **63**, 352–358 (2016).
44. Kowalczewski, C. J. *et al.* Reduction of ectopic bone growth in critically-sized rat mandible defects by delivery of rhBMP-2 from kerateine biomaterials. *Biomaterials* **35**, 3220–3228 (2014).
45. Saul, J. M., Ellenburg, M. D., de Guzman, R. C. & Van Dyke, M. Keratin hydrogels support the sustained release of bioactive ciprofloxacin. *Journal of biomedical materials research. Part A* **98**, 544–553 (2011).
46. Richter, J. R., de Guzman, R. C. & Van Dyke, M. E. Mechanisms of hepatocyte attachment to keratin biomaterials. *Biomaterials* **32**, 7555–7561 (2011).
47. Chen, J. *et al.* Synergistic enhancement of hemostatic performance of mesoporous silica by hydrocaffeic acid and chitosan. *International Journal of Biological Macromolecules* **139**, 1203–1211 (2019).
48. Liu, C. *et al.* Mussel-inspired degradable antibacterial polydopamine/silica nanoparticle for rapid hemostasis. *Biomaterials* **179**, 83–95 (2018).
49. Archana, D., Dutta, J. & Dutta, P. K. Evaluation of chitosan

- nano dressing for wound healing: Characterization, in vitro and in vivo studies. *International Journal of Biological Macromolecules* **57**, 193–203 (2013).
50. Subramanian, S., Singireddy, A., Krishnamoorthy, K. & Rajappan, M. Nanosponges: a novel class of drug delivery system--review. *Journal of pharmacy & pharmaceutical sciences* **15**, 103–111 (2012).
  51. Rawtani, D. & Agrawal, Y. K. Emerging Strategies and Applications of Layer-by-Layer Self-Assembly. *Nanobiomedicine* **1**, 8 (2014).
  52. Tan, L. *et al.* Tannic acid/Ca(II) anchored on the surface of chitin nanofiber sponge by layer-by-layer deposition: Integrating effective antibacterial and hemostatic performance. *International Journal of Biological Macromolecules* **159**, 304–315 (2020).
  53. Gao, H. *et al.* Construction of cellulose nanofibers/quaternized chitin/organic rectorite composites and their application as wound dressing materials. *Biomaterials Science* **7**, 2571–2581 (2019).
  54. Yan, T., Cheng, F., Wei, X., Huang, Y. & He, J. Biodegradable collagen sponge reinforced with chitosan/calcium pyrophosphate nanoflowers for rapid hemostasis. *Carbohydrate Polymers* **170**, 271–280 (2017).
  55. Ma, J. & Wu, C. Bioactive inorganic particles-based biomaterials for skin tissue engineering. *Exploration* 20210083 (2022).
  56. Chen, X. *et al.* Absorbable nanocomposites composed of mesoporous bioglass nanoparticles and polyelectrolyte complexes for surgical hemorrhage control. *Materials Science and Engineering C* **109**, 110556 (2020).
  57. Chen, X. *et al.* Evaluation of absorbable hemostatic agents of polyelectrolyte complexes using carboxymethyl starch and chitosan oligosaccharide both: In vitro and in vivo. *Biomaterials Science* **6**, 3332–3344 (2018).
  58. Grover, S. P. & Mackman, N. Intrinsic Pathway of Coagulation and Thrombosis. *Arteriosclerosis, thrombosis, and vascular biology* **39**, 331–338 (2019).
  59. Sundaram, M. N., Amirthalingam, S., Mony, U., Varma, P. K. & Jayakumar, R. Injectable chitosan-nano bioglass composite hemostatic hydrogel for effective bleeding control. *International Journal of Biological Macromolecules* **129**, 936–943 (2019).
  60. Borguet, Y. P. *et al.* Development of Fully Degradable Phosphonium-Functionalized Amphiphilic Diblock Copolymers for Nucleic Acids Delivery. *Biomacromolecules* **19**, 1212–1222 (2018).
  61. Samarajeewa, S. *et al.* Degradable Cationic Shell Cross-Linked Knedel-like Nanoparticles: Synthesis, Degradation, Nucleic Acid Binding, and in Vitro Evaluation. *Biomacromolecules* **14**, 1018–1027 (2013).
  62. Cho, S. *et al.* Functionalizable Hydrophilic Polycarbonate, Poly(5-methyl-5-(2-hydroxypropyl)aminocarbonyl-1,3-dioxan-2-one), Designed as a Degradable Alternative for PHMA and PEG. *Macromolecules* **48**, 8797–8805 (2015).
  63. Song, Y. *et al.* Morphologic design of silver-bearing sugar-based polymer nanoparticles for uroepithelial cell binding and antimicrobial delivery. *Nano Letters* **21**, 4990–4998 (2021).
  64. Elsbahy, M. *et al.* Differential immunotoxicities of poly(ethylene glycol)- vs. poly(carboxybetaine)-coated nanoparticles. *Journal of Controlled Release* **172**, 641–652 (2013).
  65. Elsbahy, M., Zhang, M., Gan, S. M., Waldron, K. C. & Leroux, J. C. Synthesis and enzymatic stability of PEGylated oligonucleotide duplexes and their self-assemblies with polyamidoamine dendrimers. *Soft Matter* **4**, 294–302 (2008).
  66. Elsbahy, M., Samarajeewa, S., Raymond, J. E., Clark, C. & Wooley, K. L. Shell-crosslinked knedel-like nanoparticles induce lower immunotoxicity than their non-crosslinked analogs. *Journal of Materials Chemistry B* **1**, 5241–5255 (2013).
  67. Abdelkader, A. *et al.* Ultrahigh antibacterial efficacy of meropenem-loaded chitosan nanoparticles in a septic animal model. *Carbohydrate Polymers* **174**, 1041–1050 (2017).

## Design of Nanoconstructs that Exhibit Enhanced Hemostatic Efficiency and Bioabsorbability

Rana A. Eissa<sup>1</sup>, Hesham A. Saafan<sup>1</sup>, Aliaa E. Ali<sup>2</sup>, Kamilia M. Ibrahim<sup>3</sup>, Noura G. Eissa<sup>1,4</sup>, Mostafa A. Hamad<sup>5</sup>,

Ching Pang<sup>6</sup>, Hongming Guo<sup>6</sup>, Hui Gao<sup>7\*</sup>, Mahmoud Elsabahy<sup>1,6,8\*</sup> and Karen L. Wooley<sup>6\*</sup>

<sup>1</sup>School of Biotechnology and Science Academy, Badr University in Cairo, Badr City, Cairo 11829, Egypt

<sup>2</sup>Department of Chemistry, University of Turku, Vatselankatu 2, 20014 Turku, Finland

<sup>3</sup>Department of Pharmacology, Faculty of Pharmacy, Ain Shams University, Cairo 11561, Egypt

<sup>4</sup>Department of Pharmaceutics and Industrial Pharmacy, Faculty of Pharmacy, Zagazig University, Zagazig 44519, Egypt

<sup>5</sup>Department of Surgery, Faculty of Medicine, Assiut University, Assiut 71515, Egypt

<sup>6</sup>Departments of Chemistry, Chemical Engineering, and Materials Science & Engineering, Texas A&M University, College Station, Texas 77842, USA

<sup>7</sup>State Key Laboratory of Separation Membranes and Membrane Processes, School of Materials Science and Engineering, Tiangong University, Tianjin 300387, P. R. China

<sup>8</sup>Misr University for Science and Technology, 6th of October City, Cairo 12566, Egypt

\*Corresponding authors: [hui.gao@tiangong.edu.cn](mailto:hui.gao@tiangong.edu.cn); [wooley@chem.tamu.edu](mailto:wooley@chem.tamu.edu); [mahmoud.elsabahy@buc.edu.eg](mailto:mahmoud.elsabahy@buc.edu.eg)

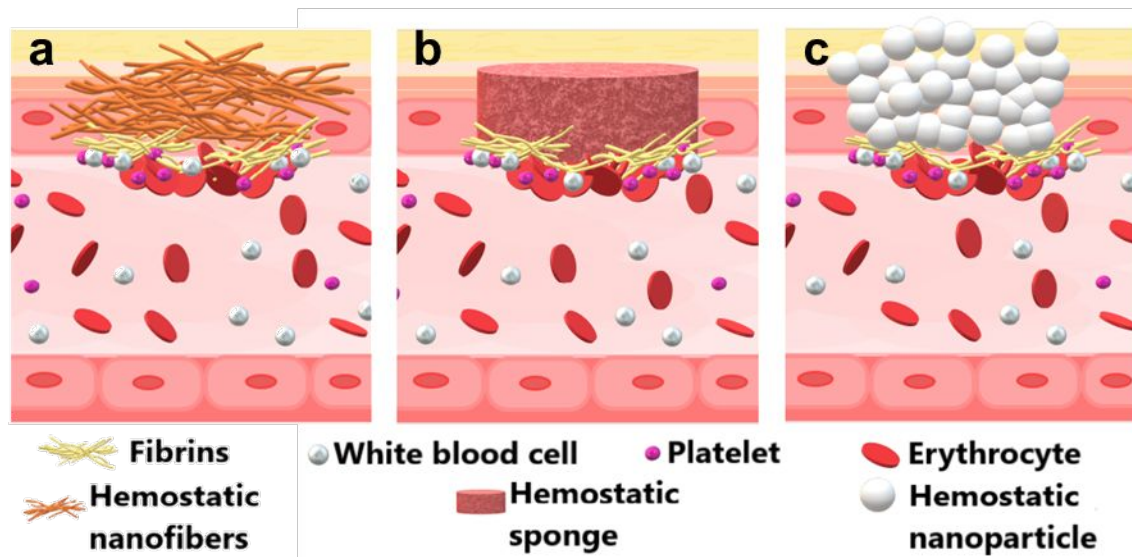


**Fig. 1.** Degradable hemostatic nanocomposites could be constructed as (a) nanofibers, (b) nano-sponges, and (c) nanoparticles, of various compositions and characteristics. Hemostatic nanocomposites aggregate and trap red blood cells and platelets in the wound site, thereby, enhancing and accelerating the blood clotting process.

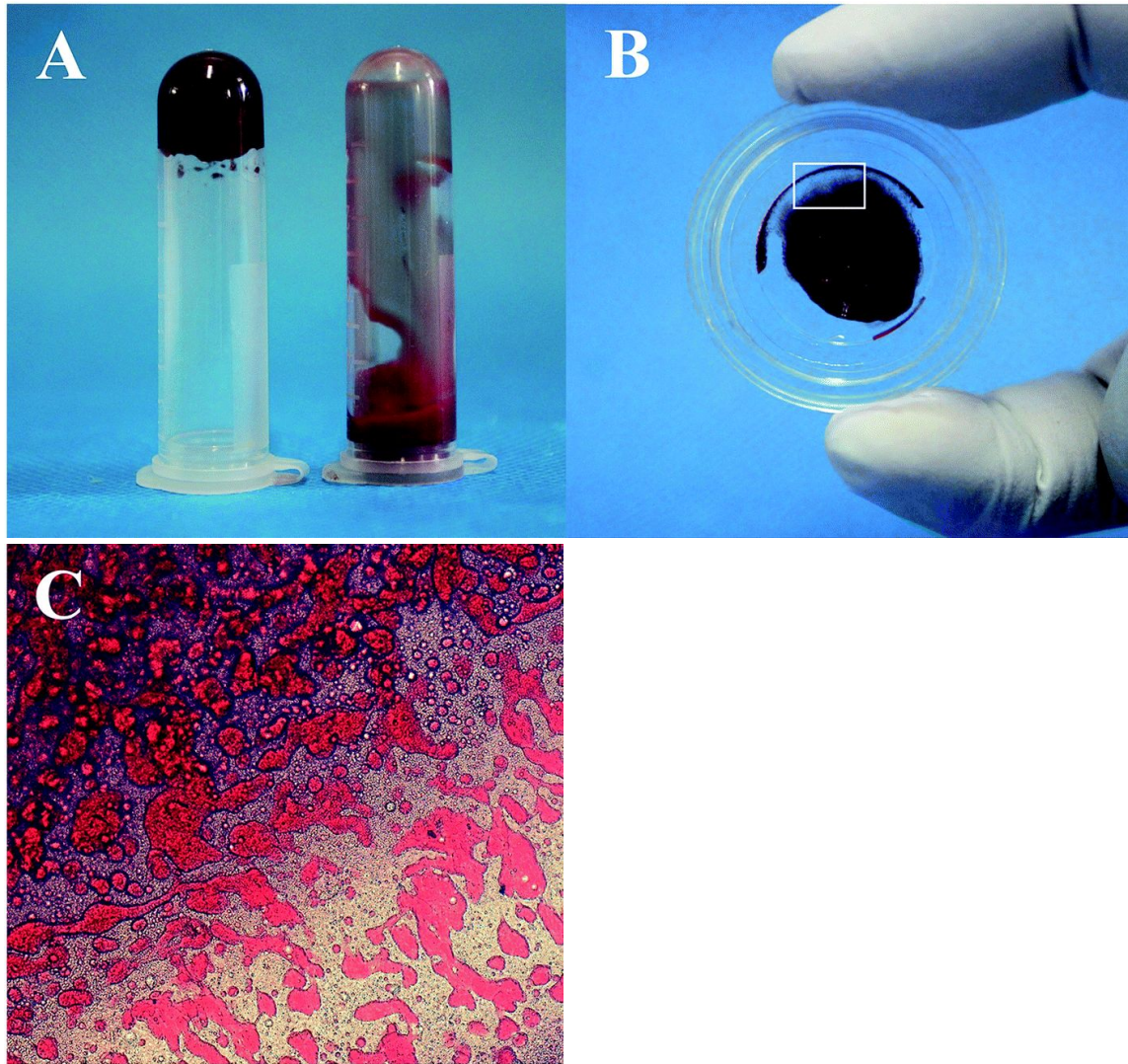


**Fig. 2.** (A) Formation of blood clot in vitro (left: CCM/MSNs-PVP; right: common hemostatic gauze). (B) Formation of the hydrogel composite. (C) Microscopic image of the hydrogel composite structure. This figure has been adapted from ref [38] with permission from Royal Society of Chemistry, copyright 2022, <https://creativecommons.org/licenses/by/3.0/>.

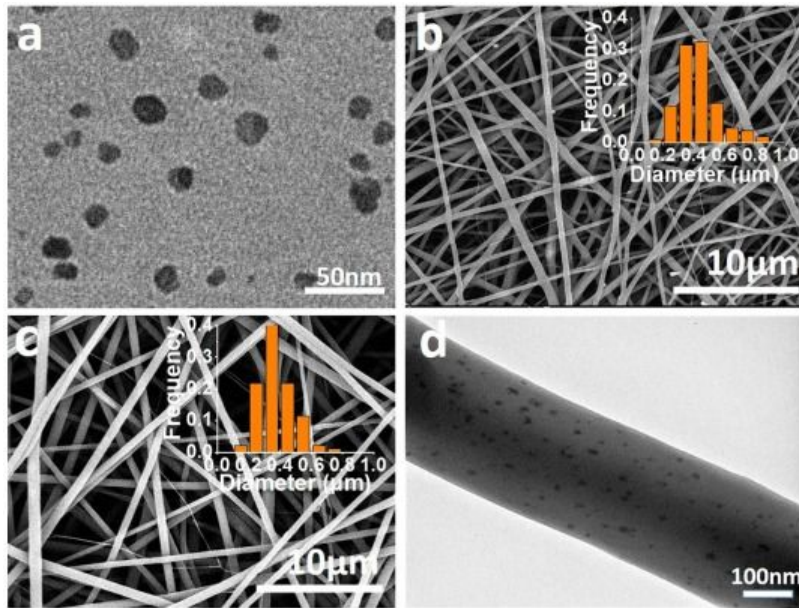


**Fig. 3.** (a) TEM image of CuS nanoparticles. (b and c) SEM images of different concentrations of CuS composite nanofibers. (d) TEM image of CuS nanofiber. This figure has been reproduced from ref [40] with permission from Elsevier, copyright 2022.

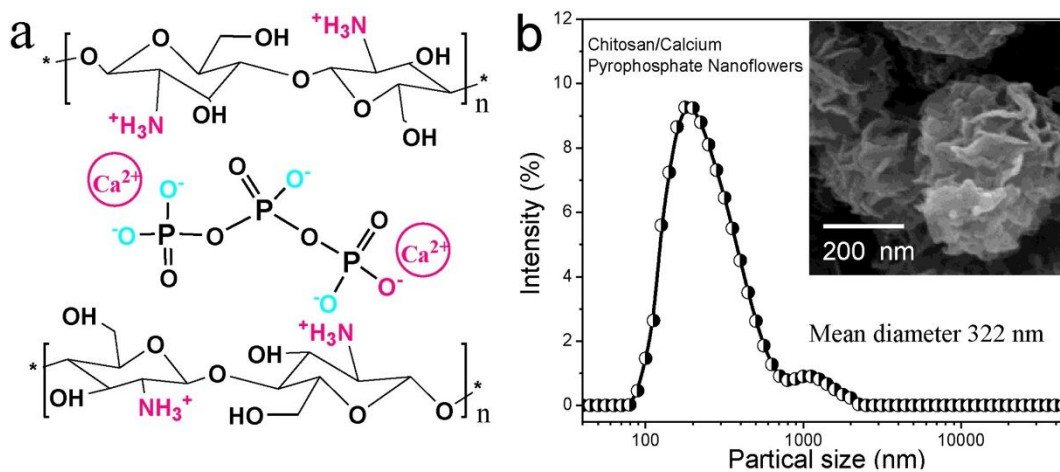


**Fig. 4.** (a) Chemical structure of CPNFs, synthesized by a one-pot preparation method. (b) The particle size distribution and SEM image (inset) of the CPNFs. This figure has been reproduced from ref [54] with permission from Elsevier, copyright 2022.

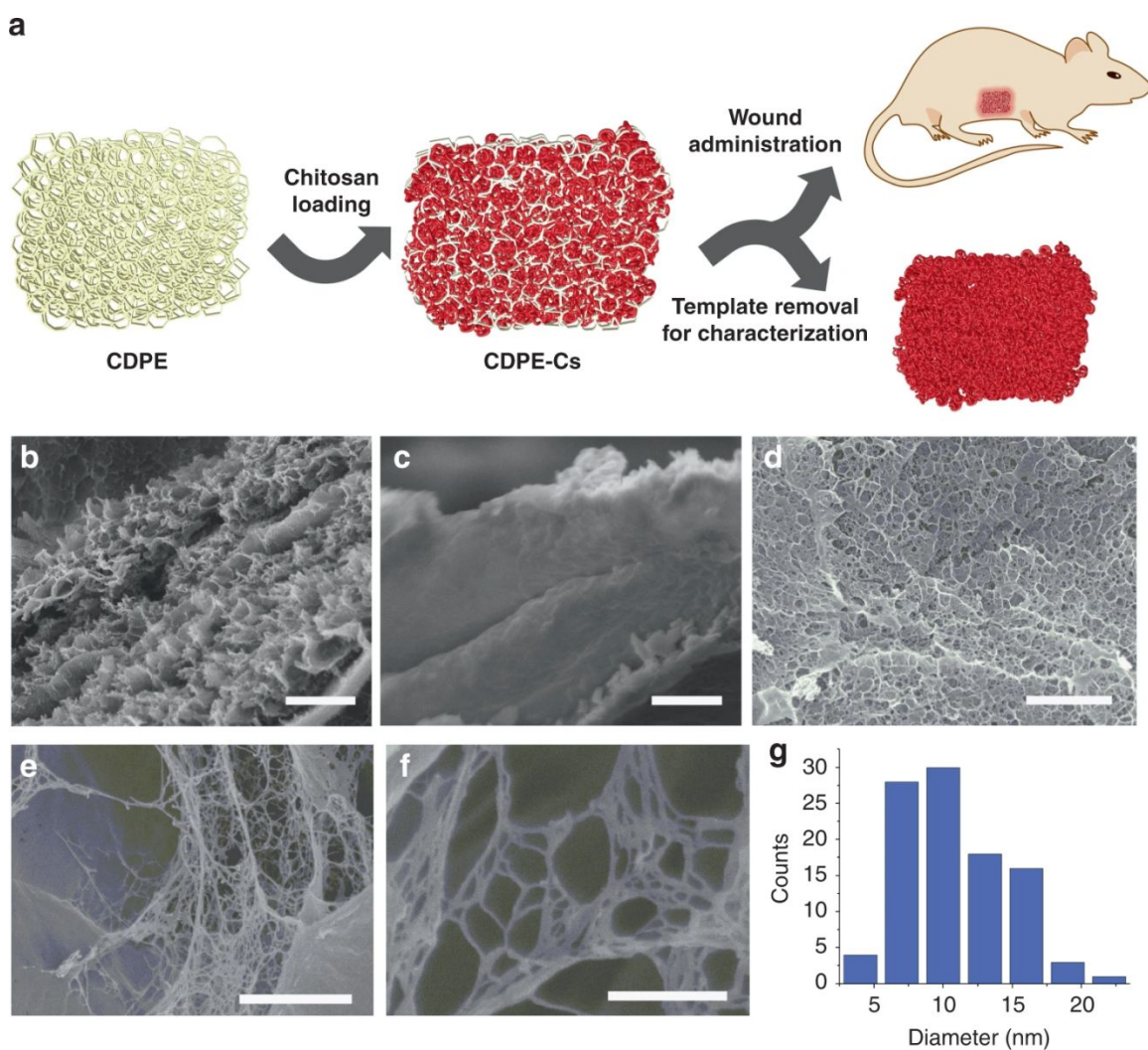


**Fig. 5.** Prepared materials exhibit amorphous, macroporous morphology. (a) Simplified illustration of the chitosan templating process, administration of CDPE-Cs to wound site, and template removal for imaging. (b) SEM image of CDPE after drying by lyophilization, showing complex, porous morphology (scale bar is 2  $\mu\text{m}$ ). (c) SEM image of chitosan-loaded composite CDPE-Cs gel after lyophilization (scale bar is 2  $\mu\text{m}$ ). (d) SEM image of templated chitosan material, displaying a honeycomb-like structure (scale bar is 2  $\mu\text{m}$ ). (e–f) Magnified SEM images of nanofibrillar domains in the templated chitosan, with a web-like morphology within the network cavities (scale bars are 500 nm and 300 nm, respectively). (g) Histogram plot showing the distribution of fiber diameters measured by SEM. This figure has been reproduced from ref [8] with permission from Nature Portfolio, copyright 2022, <http://creativecommons.org/licenses/by/4.0/>.

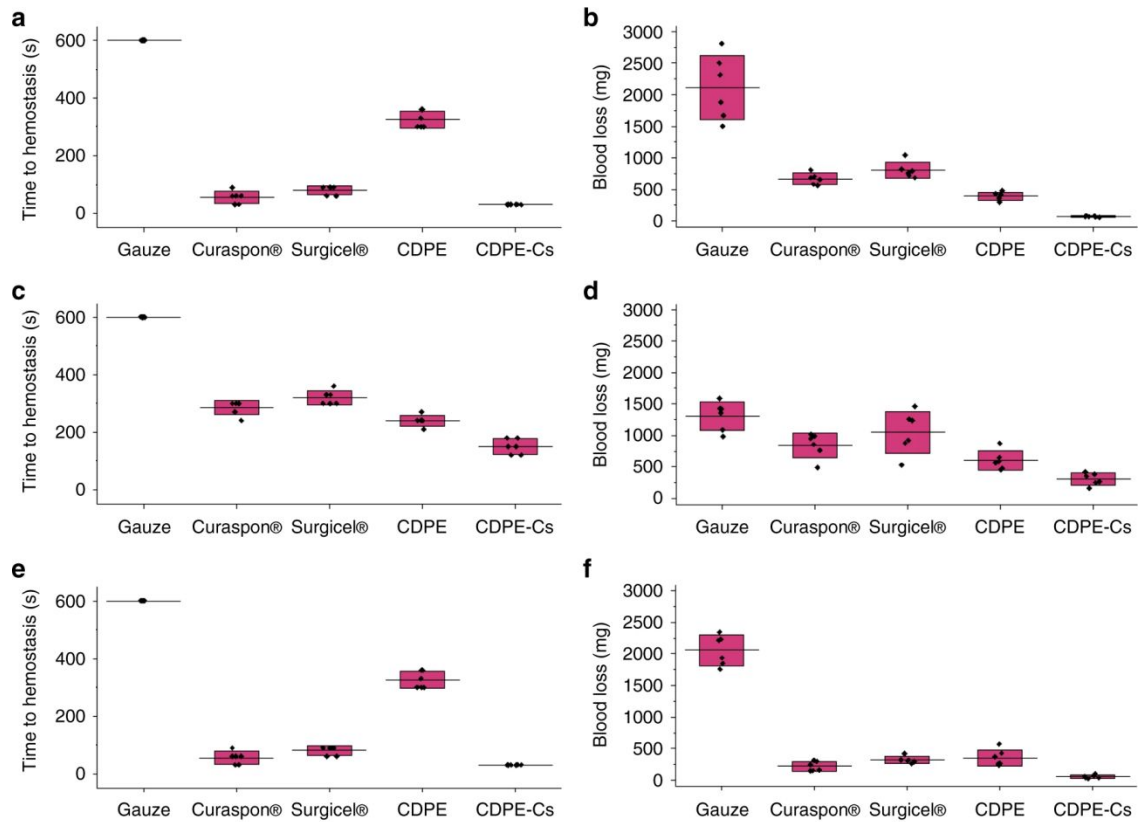


**Fig. 6.** *In vivo* examination of CDPE-Cs hydrogels against several controls. (a) Conventional gauze dressings, Curaspon®, Surgicel®, and CDPE and CDPE-Cs hydrogels were applied immediately after induction of the liver injury and absorption of the initial bleeding from the injury sites, to determine the total time to hemostasis in rats ( $n = 6$  animals per group). For gauze dressings, bleeding did not stop until the end of experiments (600 s). (b) The total amount of blood loss, measured over 10 min, in rats ( $n = 6$  animals per group). (c) Time to hemostasis for rabbits ( $n = 6$  animals per group). (d) Blood loss in rabbits ( $n = 6$  animals per group). (e) Time to hemostasis for pigs ( $n = 6$  animals per group). (f) Blood loss in pigs ( $n = 6$  animals per group). Box plots correspond to means (center line)  $\pm$  SD (boundaries). This figure has been reproduced from ref [8] with permission from Nature Portfolio, copyright 2022, <http://creativecommons.org/licenses/by/4.0/>.